

Computing Quasi-Normal Modes of Schwarzschild Black Holes with Physics-Informed Neural Networks

Supervisor Progress Presentation

Jonathan Chung

University of Cambridge

25 February 2026

Outline

- 1 Black Hole Ringdown & the Master Equation
- 2 Methodology: PINNs & Finite Differences
- 3 Results

What Are Quasi-Normal Modes?

- A perturbed Schwarzschild black hole emits gravitational radiation as it settles down — the **ringdown**.
- The ringdown consists of **quasi-normal modes** (QNMs): damped sinusoids

$$\Phi(t) \propto e^{-t/\tau} \cos(\omega t)$$

- The frequency ω and decay time τ depend **only on the black hole mass M** (for Schwarzschild).
- **Goal:** Solve the perturbation equations numerically to extract ω and τ .

From Einstein's Equations to a Master Equation

Start with the Schwarzschild metric and add a small perturbation:

$$g_{\mu\nu} = g_{\mu\nu}^0(\text{Schwarzschild}) + h_{\mu\nu}(\text{small})$$

Key simplifications:

- ① Linearise Einstein's equations in $h_{\mu\nu}$.
- ② Decompose $h_{\mu\nu}$ in **tensor spherical harmonics** — angular dependence separates.
- ③ Construct a gauge-invariant **master function** Φ from the metric perturbation components.

Result: a single 1+1D wave equation for each angular mode ℓ :

$$\boxed{-\frac{\partial^2 \Phi}{\partial t^2} + \frac{\partial^2 \Phi}{\partial x^2} - V(r) \Phi = 0}$$

where $x = r + 2M \ln\left(\frac{r}{2M} - 1\right)$ is the **tortoise coordinate**.

The Potentials

The potential $V(r)$ depends on the **parity** of the perturbation:

Odd-parity (axial) — Regge–Wheeler:

$$V_{\text{RW}} = \left(1 - \frac{2M}{r}\right) \left[\frac{\ell(\ell+1)}{r^2} - \frac{6M}{r^3} \right]$$

Even-parity (polar) — Zerilli:

$$V_{\text{Z}} = \left(1 - \frac{2M}{r}\right) \frac{2n^2(n+1)r^3 + 6n^2Mr^2 + 18nM^2r + 18M^3}{r^3(nr+3M)^2}$$

where $2n = (\ell - 1)(\ell + 2)$.

- Both potentials peak near $x \sim 1M$ and vanish at the horizon and infinity.
- A transformation connects them (Chandrasekhar) \Rightarrow **same QNMs**.
- We focus on the **Zerilli potential** with $\ell = 2$ (dominant mode).

Boundary & Initial Conditions

Boundary conditions (Sommerfeld — radiation conditions):

$$\text{Horizon } (x \rightarrow -\infty) : (\partial_t - \partial_x) \Phi = 0 \quad (\text{ingoing})$$

$$\text{Infinity } (x \rightarrow +\infty) : (\partial_t + \partial_x) \Phi = 0 \quad (\text{outgoing})$$

Initial conditions — outgoing Gaussian pulse:

$$\Phi(x, 0) = \exp \left[-\frac{(x - 4M)^2}{(5M)^2} \right]$$

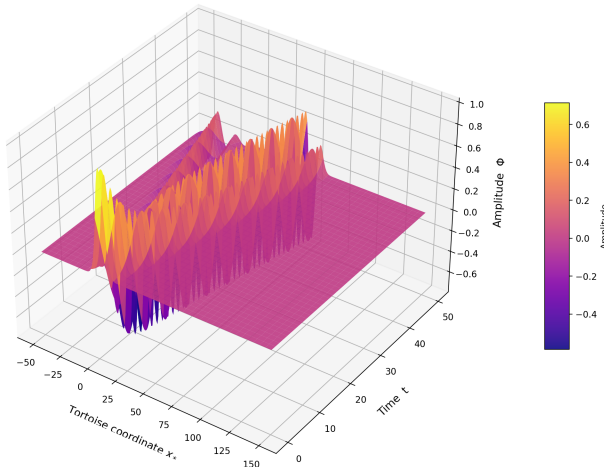
$$\partial_t \Phi(x, 0) = -\partial_x \Phi(x, 0) \quad (\text{purely right-moving})$$

Domain: $x/M \in [-50, 150]$, $t/M \in [0, 50]$.

The pulse scatters off the potential barrier \Rightarrow ringdown at late times.

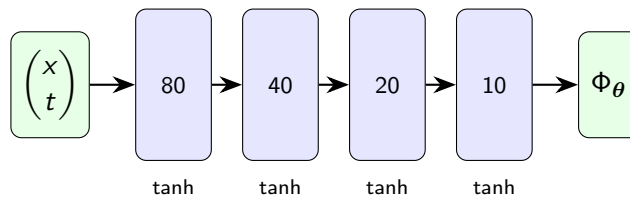
Ringdown Waveform — 3D Visualisation

3D Waveform of Schwarzschild Black Hole Ringdown (FD Reference)



Physics-Informed Neural Networks — Core Idea

Instead of a grid, train a neural network $\Phi_\theta(x, t)$ to satisfy the PDE, BCs, and ICs simultaneously.



- 4 hidden layers, tanh activation, Glorot uniform initialisation.
- Output transform: $\Phi_\theta = \text{Atanh}(\text{raw output})$ bounds the solution to $[-1, 1]$.
- Derivatives via **automatic differentiation** (exact, no discretisation error).
- **4,521 trainable parameters.**

The Loss Function

Train by minimising a weighted sum of 7 terms:

$$\mathcal{L} = \lambda \cdot \left[\underbrace{\mathcal{L}_r, \mathcal{L}_{r_x}, \mathcal{L}_{r_t}}_{\text{PDE residual}}, \underbrace{\mathcal{L}_{ic}, \mathcal{L}_{iv}}_{\text{initial condns.}}, \underbrace{\mathcal{L}_{bl}, \mathcal{L}_{br}}_{\text{boundary condns.}} \right]$$

Term	Penalises	Points
\mathcal{L}_r	$\Phi_{tt} - \Phi_{xx} + V\Phi \neq 0$	$N_r = 32,000$
$\mathcal{L}_{r_x}, \mathcal{L}_{r_t}$	Gradients of residual (gradient-enhanced PINN)	same
$\mathcal{L}_{ic}, \mathcal{L}_{iv}$	Initial profile & velocity mismatch	$N_i = 800$
$\mathcal{L}_{bl}, \mathcal{L}_{br}$	Sommerfeld BC violations	$N_b = 400$

- **Phase problem:** $\Phi(x, t + \alpha)$ is also a solution \Rightarrow weight λ_{iv} heavily to lock the correct phase.
- Total: **33,600 collocation points** (vs. 500,000 grid points for FD).

Two-Phase Training

Phase 1: Adam (10,000 iters)

- Stochastic gradient descent with adaptive learning rate ($\text{lr} = 10^{-3}$).
- Good at rough, global exploration.
- Uniform point resampling every 100 iters.

Phase 2: L-BFGS (15,000 iters)

- Quasi-Newton: approximates inverse Hessian from gradient history.
- Fast, precise convergence near minima.
- Sensitive to point changes \Rightarrow only uniform resampling here.



Finite Difference Baseline

For comparison, we solve the same PDE with standard numerical methods:

- Uniform mesh: $N_x = 1,000$ points, $\Delta x = 0.2M$.
- Method of lines + 4th-order Runge–Kutta, $\Delta t = 0.1M$.
- 500 time steps $\Rightarrow N_F = 500,000$ grid points.

The FD solution serves as **ground truth** for evaluating the PINN.

Key comparison:

	FD	PINN
Representation	Grid values $\Phi_{i,j}$	Neural network $\Phi_\theta(x, t)$
Derivatives	FD stencils (approx.)	Autograd (exact)
Points	500,000	33,600
Time-stepping	Explicit RK4	None (global solve)

Extracting Quasi-Normal Modes

Sample $\Phi(x_q, t)$ at observation point $x_q = 10M$, restrict to late times.

Method 1 — FFT + Envelope:

- ω : FFT of $\Phi(x_q, t) \Rightarrow$ peak frequency.
- τ : Linear fit to $\ln |\text{envelope peaks}|$ vs. $t \Rightarrow$ slope $= -1/\tau$.

Method 2 — Direct curve fit:

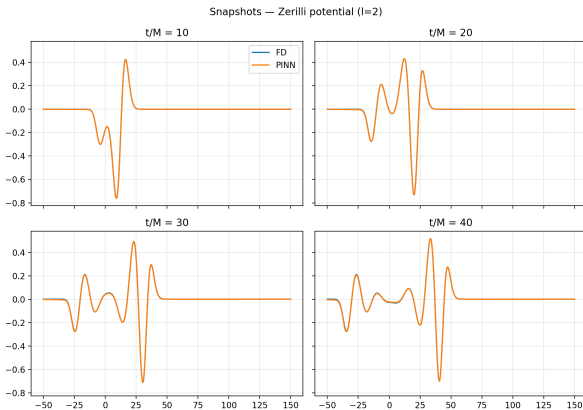
- Fit $\Phi \approx A e^{-t/\tau} \cos(\omega t + \phi)$ directly via nonlinear least squares.

Compare extracted (ω, τ) against theoretical values (Leaver 1985):

ℓ	ωM	τ/M
2	0.3737	11.241

Paper Reproduction: Baseline Results

Reproduced the setup of Patel, Aykutalp & Laguna (2024) with our corrected outgoing initial velocity profile.



Zerilli $\ell = 2$ QNM Extraction

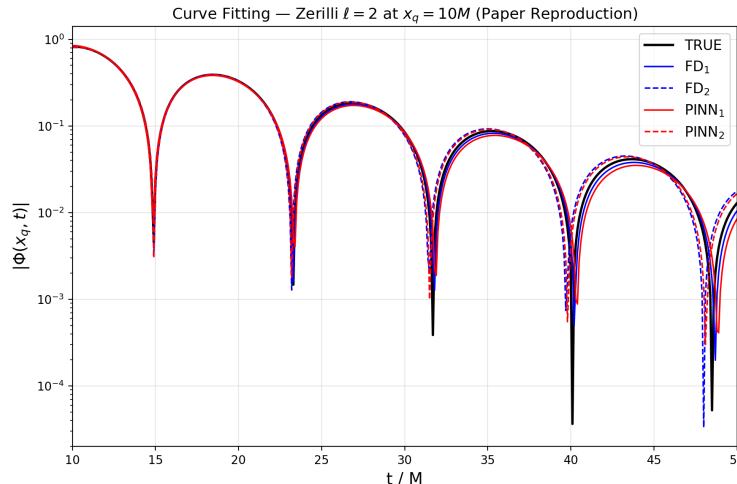
	τ/M	ωM
TRUE	11.241	0.3737
FD₁	10.929 (2.78)	0.3716 (0.56)
FD₂	11.465 (2.00)	0.3798 (1.63)
PINN₁	10.671 (5.07)	0.3697 (1.08)
PINN₂	11.410 (1.50)	0.3784 (1.25)

Parentheses: % error vs. Leaver 1985.

Subscript 1 = FFT + envelope.

Subscript 2 = direct curve fit.

Curve Fitting — Paper Reproduction



$\log |\Phi|$ vs. t/M at $x_q = 10M$. All five reconstructed damped cosines $A e^{-t/\tau} \cos(\omega t + \phi)$ overlap closely — both FD and PINN extract QNMs within $\sim 1\text{--}4\%$ of the Leaver (1985) values.

QNM Accuracy: Our Results vs. the Paper

Zerilli $\ell = 2$ — τ/M and ωM percentage errors

	Paper (Patel et al.)		Ours	
	τ/M (% err)	ωM (% err)	τ/M (% err)	ωM (% err)
FD ₁	10.804 (3.89)	0.370 (0.90)	10.929 (2.78)	0.372 (0.56)
FD ₂	11.073 (1.49)	0.378 (1.26)	11.465 (2.00)	0.380 (1.63)
PINN ₁	10.089 (10.25)	0.375 (0.29)	10.671 (5.07)	0.370 (1.08)
PINN ₂	9.620 (14.42)	0.376 (0.52)	11.410 (1.50)	0.378 (1.25)

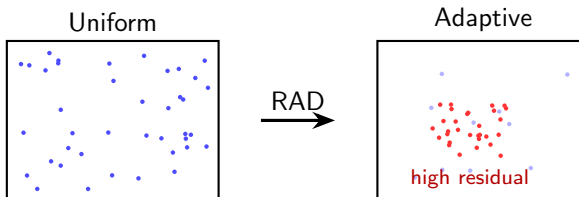
- **Major improvement:** PINN₂ decay time error drops from **14.42%** → **1.50%** (**9.6**× more accurate).
- PINN₁ τ error also improves: 10.25% → 5.07% (2.0×).
- Likely cause: our corrected outgoing initial velocity $\partial_t \Phi = -\partial_x \Phi$ (Sommerfeld condition).

Our Improvement: Residual-Adaptive Distribution (RAD)

Problem: Uniform sampling wastes points in empty regions where $\Phi \approx 0$.

RAD (Wu et al. 2023): Every P training steps during Adam—

- ① Generate 100,000 random candidate points.
- ② Evaluate PDE residual $|r_i|$ at each candidate.
- ③ Compute sampling probability: $p_i \propto |r_i|^k + c$.
- ④ Sample 32,000 points from candidates \Rightarrow replace all domain points.

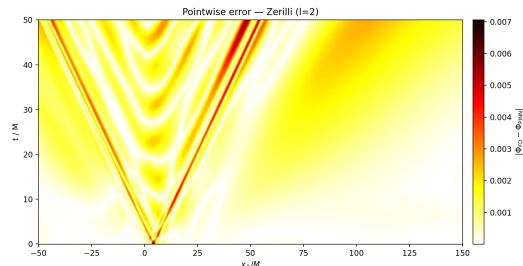
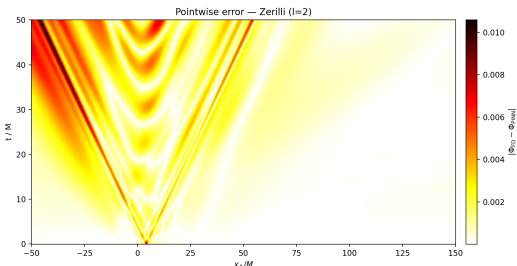


RAD Tuning Experiments

Configuration	k	c	Final Loss	RMSD	RL2
Uniform (paper repro)	—	—	1.18×10^{-6}	0.00183	1.30%
RAD baseline	1	1	7.40×10^{-7}	0.00115	0.82%
RAD aggressive	2	0.1	9.07×10^{-7}	0.00095	0.67%
RAD $k=2, P=500$	2	0.1	1.06×10^{-6}	0.00105	0.75%
RAD + anchor (20%)	1	1	8.20×10^{-7}	0.00141	1.00%

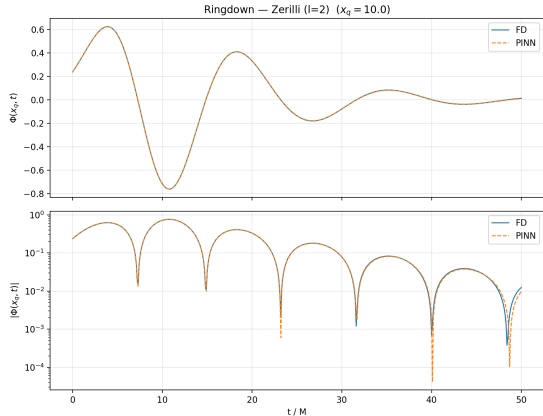
- RAD reduces RMSD by **37%** over uniform sampling.
- Aggressive RAD ($k=2$) achieves the **best RMSD** (0.00095).
- Anchor retention has the **second-lowest loss** (8.20×10^{-7}) but the **highest RMSD** among RAD runs — suggests over-fitting to anchor points at the expense of global accuracy.

Spatial Error Distribution

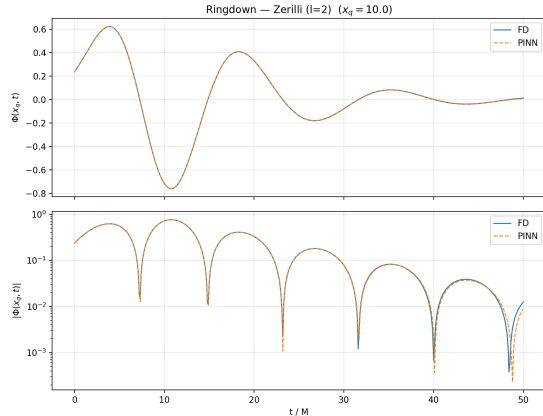


RAD reduces the error concentration at the **wavefront leading edge**.

Ringdown Waveform at $x_q = 10M$



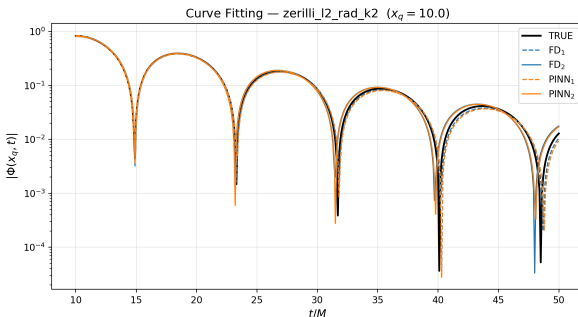
RAD baseline: PINN vs. FD (raw waveforms)



RAD $k = 2$: PINN vs. FD (raw waveforms)

Top: linear scale; Bottom: $\log |\Phi|$. Both variants closely match the FD reference.

Curve Fitting — RAD $k=2$



$\log |\Phi|$ vs. t/M at $x_q = 10M$ (RAD $k=2$)

Zerilli $\ell = 2$ — QNM Extraction

	τ/M	ωM
TRUE	11.241	0.3737
FD₁	10.929 (2.78)	0.3716 (0.56)
FD₂	11.465 (2.00)	0.3798 (1.63)
PINN₁	10.831 (3.65)	0.3705 (0.85)
PINN₂	11.443 (1.80)	0.3790 (1.43)

FD_{1,2} identical to paper repro
(same FD solver).

PINN_{1,2} from RAD $k=2$ run.

- RAD PINN₂: τ error 1.80% vs. 1.50% (paper repro) — comparable accuracy.
- RAD primarily improves **spatial** accuracy (RMSD), not QNM extraction.

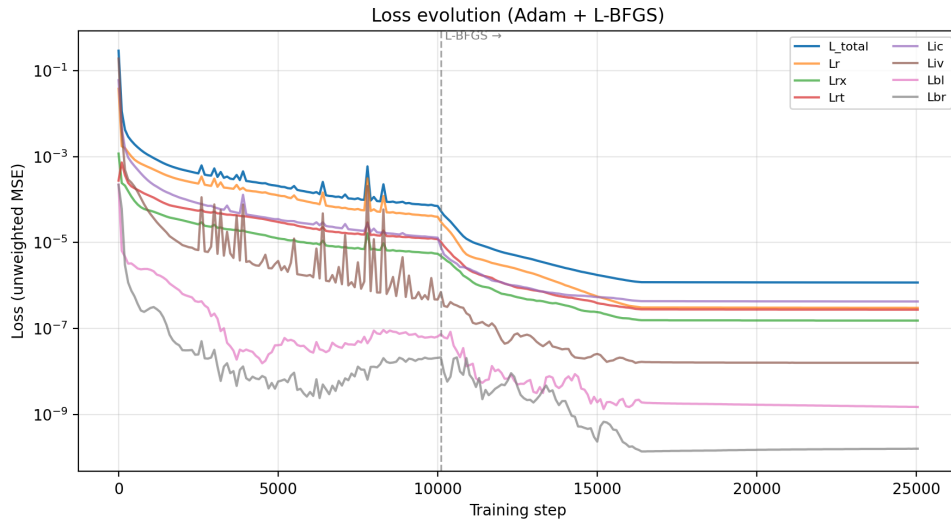
Summary of Findings

- ① **PINNs can compute QNMs** of Schwarzschild black holes to within $\sim 1\text{--}2\%$ of known values, using $15\times$ fewer collocation points than FD.
- ② **RAD adaptive sampling** improves solution accuracy by $\sim 37\%$ (RMSD) over uniform sampling, by concentrating points where the PDE residual is largest.
- ③ **Aggressive RAD** ($k = 2$) provides the best spatial accuracy (lowest RMSD/RL2). Anchor retention has the second-lowest loss but the highest RMSD among RAD runs — over-fitting to anchor points.
- ④ **Exponential reweighting fails** — naively amplifying late-time residuals destabilises training (τ error $> 20\%$).

Thank you

Questions?

Appendix: Loss History — Reproduction Run (Uniform Sampling)



Appendix: Loss History — RAD Adaptive Sampling

